Catalysis Today 152 (2010) 11–16

Contents lists available at ScienceDirect

Catalysis Today

journal homepage: www.elsevier.com/locate/cattod

Acidity and accessibility studies on mesoporous ITQ-4 zeolite

Danny Verboekend[a], Luis A. Villaescusa[b], Karine Thomas[c], Irina Stan[c], Javier Pérez-Ramírez[a,d,*]

[a] Institute of Chemical Research of Catalonia (ICIQ), Avinguda Països Catalans 16, 43007 Tarragona, Spain
[b] Instituto de Reconocimiento Molecular y Desarrollo Tecnológico (IDM). Centro mixto Universidad Politécnica de Valencia-Universidad de Valencia. Departamento de Química, Universidad Politécnica de Valencia, Camino de Vera s/n, 46022, Valencia, Spain
[c] Laboratoire Catalyse et Spectrochimie, ENSICAEN, Université de Caen, CNRS, 6 Bd du Maréchal Juin, 14050 Caen, France
[d] Catalan Institution for Research and Advanced Studies (ICREA), Passeig Lluís Companys 23, 08010 Barcelona, Spain

ARTICLE INFO

Article history:
Available online 7 March 2010

Keywords:
Hierarchical zeolites
ITQ-4
Desilication
Mesopores
Acidity
Accessibility

ABSTRACT

Desilication of ITQ-4 (IFR code, 1-dimensional 12-MR channel system of 0.62 nm × 0.72 nm) in aqueous NaOH solutions was practiced in order to produce the zeolite in the hierarchical form, *i.e.* combining the native micropores with a secondary network of intracrystalline mesopores. The parent material (Si/Al = 32) was synthesized using benzylquinuclidinium as the structure-directing agent in the presence of fluoride anions. The samples were characterized by ICP-OES, XRD, TEM, N_2 adsorption, and FTIR spectroscopy. In a representative treatment, the mesopore surface area of the ITQ-4 experienced a sevenfold increase (from 29 to 206 $m^2\ g^{-1}$) upon optimized NaOH post-treatment, whereas the microporosity was reduced by 70% (from 0.20 to 0.06 $cm^3\ g^{-1}$). Chemical analysis and infrared spectroscopy of adsorbed pyridine showed that after alkaline treatment the amount of Brønsted acid sites remains practically constant whereas a significant increase in Lewis acid sites was obtained. Infrared studies with adsorbed 2,4,6-collidine concluded that the accessibility of acid sites in the hierarchical zeolite increased substantially due to an increase in the available active sites at the pore mouths of the hierarchical zeolite.

1. Introduction

The synthesis of new zeolitic materials is an important field of research due to the potential applications of new structures or compositions in catalysis, separation, and adsorption processes. In recent years, substantial efforts have been devoted to the design of zeolites with improved accessibility and molecular transport to/from the active sites. By doing this, diffusion limitations can be alleviated enabling improved catalytic performance in known as well as in novel reactions. Wide-pore zeolites with a multidirectional channel system and hierarchical zeolites combining the native microporosity with a secondary network of mesopores [1] comprise the two basic families of materials promising enhanced zeolite effectiveness in catalysis by increasing the diffusivity or by shortening the diffusion pathlength, respectively.

The controlled extraction of framework silicon by treatment in aqueous NaOH is widely used to introduce mesoporosity in various zeolite frameworks: MFI [2], MTW [3], MOR [4], AST [5], BEA [6], and FER [7]. Although the benefits of mesoporosity to the catalytic performance of the above zeolites have been unequivocally proven [1], there is a lack of detailed studies assessing the accessibility and diffusion of molecules in hierarchical zeolites, as well as changes in acidic properties induced by the post-synthesis treatment. The scarce literature available in this respect mainly deals with ZSM-5 [8–12]. Recently, some of us have shown that infrared spectroscopy of substituted alkylpyridines with different sizes (pyridine, 2,6-lutidine, and 2,4,6-collidine) enables to quantify the remarkably enhanced accessibility of acid sites in mesoporous ZSM-5 with respect to the purely microporous counterpart [11]. The derived accessibility index (ACI) can be used to standardize acid site accessibility in zeolites.

It is relevant to expand the number of zeolite families that can be prepared in hierarchical form. Special attention should be placed on zeolites with small micropores and/or one-dimensional channel systems as they suffer to a more pronounced extent from diffusion constraints in catalytic applications. We have drawn our attention to ITQ-4 (IFR topology), which is isotypical with SSZ-42 and MCM-58 [13]. The ITQ-4 structure comprises a monoclinic framework and is characterized by a high void volume and by its unique 1-dimensional sinusoidal 12-membered ring channel system (Fig. 1). Villaescusa et al. [14] reported the synthesis of ITQ-4 in the Si/Al range of 20-∞ and the physico-chemical characterization of the as-made and calcined materials.

* Corresponding author at: Institute for Chemical and Bioengineering, Department of Chemistry and Applied Biosciences, ETH Zurich, Wolfgang-Pauli-Strasse 10, CH-8093 Zurich, Switzerland. Tel.: +41 44 633 7120; fax: +41 44 633 1405.
E-mail address: jpr@chem.ethz.ch (J. Pérez-Ramírez).

0920-5861/$ – see front matter © 2010 Elsevier B.V. All rights reserved.
doi:10.1016/j.cattod.2010.02.004

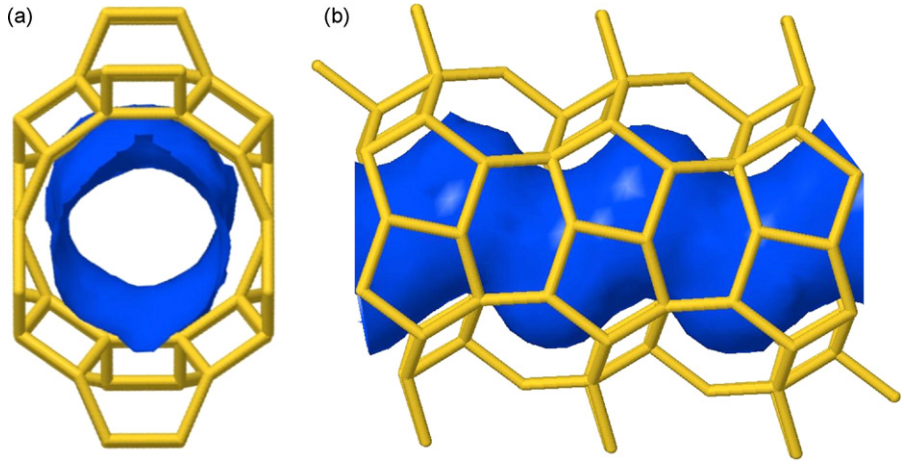

Fig. 1. Representation of the IFR framework: (a) along [0 0 1] visualizing the 12-MR channels of 0.62 nm × 0.72 nm and (b) along [0 1 0] visualizing the sinusoidal propagation of the pores [13].

Herein we have synthesized ITQ-4 crystals (Si/Al = 32) using benzylquinuclidium as the structure-directing agent in the presence of fluoride anions. The resulting zeolite was calcined and desilicated under various conditions in aqueous NaOH to develop different degrees of mesoporosity. The samples were characterized by ICP-OES, XRD, TEM, N_2 adsorption, and FTIR spectroscopy. This study focuses on the acidic properties and accessibility of the acid sites in the purely microporous and mesoporous hierarchical ITQ-4 samples. For this purpose, the acidic properties of both zeolites were studied by infrared spectroscopy before and after adsorption of pyridine and collidine.

2. Experimental

2.1. Synthesis of ITQ-4

The ITQ-4 zeolite with nominal Si/Al ratio of 30 was basically prepared following the recipe reported in [14]. Accordingly, 1.50 g $Al(NO_3)_3{\cdot}9H_2O$ was dissolved in 273.83 g of a basic solution of benzylquinuclidinium (BzQ) hydroxide (2.66×10^{-4} mol OH^- g^{-1} solution). Then, 23.33 g of tetraethyl orthosilicate (TEOS) was added and allowed to hydrolyze at room temperature until 240 g of solvent (water and ethanol) had evaporated. Zeolite beta can also be formed during synthesis either when Al is present in the gel or when the gel is very concentrated. Therefore, to prevent the formation of zeolite beta, crystallization promoters in the form of 0.36 g of calcined ITQ-4 (Si/Al = 30) were used. These crystals were suspended in 7.72 g of water, sonicated, added to the synthesis gel, and thoroughly mixed manually. Next, 2.39 g of HF (48% in mass) was added under magnetic stirring until the mixture became too viscous to be stirred magnetically. Then the homogenization was carried out manually. The molar gel composition per mol of SiO_2 was SiO_2:0.033AlO_2BzQ:0.5BzQF:0.1BzQNO_3:15H_2O. The gel was distributed in 22 cm^3 Teflon-lined steel autoclaves allowing it to react under static conditions at 150 °C for 13 days. Autoclaves were then quenched in cold water, after which the obtained product (pH ~7.5) was filtered, washed, and dried at 60 °C. White solids were obtained with a yield of 13.4 g of zeolite per 100 g of gel. The as-synthesized zeolite was calcined in static air at 600 °C for 5 h using a heating rate of 3 °C min^{-1} to obtain the parent (P) ITQ-4 zeolite.

2.2. Alkaline treatment

Alkaline treatments of the parent zeolite in aqueous NaOH solutions were conducted following the protocol detailed elsewhere [15] using different conditions: AT-1 (0.2 M, 65 °C, 10 min), AT-2 (0.2 M, 65 °C, 30 min), and AT-3 (0.4 M, 65 °C, 30 min). The standard conditions (AT-2) were considered optimal for the preparation of mesoporous ZSM-5 with the same Si/Al ratio range [15]. The NaOH-treated zeolites were transformed into the ammonium form via three successive exchanges in 0.1 M NH_4NO_3 aqueous solution. Finally the ammonium form was converted to the protonic form by calcination following the program described for the as-synthesized sample.

2.3. Characterization

Si and Al concentrations in the zeolites and in the filtrates of the alkaline treatment were determined by inductively coupled plasma-optical emission spectroscopy (ICP-OES) (PerkinElmer Optima 3200RL). X-ray diffraction (XRD) patterns were measured in a Siemens D5000 diffractometer with Bragg–Brentano geometry and Ni-filtered CuK_α radiation (λ = 0.1541 nm). Data were recorded in the 2θ range 5–30° with an angular step size of 0.05° and a counting time of 8 s per step. Transmission electron microscopy (TEM) was carried out in a JEOL JEM-1011 microscope operated at 100 kV. Nitrogen adsorption at −196 °C was performed in a Quantachrome Quadrasorb-SI gas adsorption analyzer. Prior to the measurement, the samples were evacuated at 350 °C for 12 h. The BET method [16] was applied to calculate the total surface area, which can be used for comparative purposes. The *t*-plot method [17] was used to discriminate between micro- and mesoporosity. The mesopore size distribution was obtained by the BJH model [18] applied to the adsorption branch of the isotherm. Infrared spectra were recorded with a Nicolet Magna 550-FTIR spectrometer at 2 cm^{-1} optical resolution, with one level of zero-filling for the Fourier transform. Prior to the measurements, the samples were pressed in self-supporting discs of *ca.* 10 mg (diameter: 1.6 cm, 5 mg cm^{-2}) and activated in the IR cell at 450 °C for 5 h down to 10^{-4} Pa. Adsorption of pyridine and collidine was performed at room temperature. A pressure of *ca.* 100 Pa was established in the cell to reach saturation followed by evacuation at 200 °C to remove physically adsorbed species. All spectra were normalized to 10 mg wafers. Difference spectra were obtained by subtracting the spectrum of the zeolite before adsorption of the probe molecule.

3. Results and discussion

3.1. Parent ITQ-4

ICP-OES analysis (Table 1) concluded that the metal incorporation in the solid was performed accurately as the obtained Si/Al

Table 1
Characterization of the parent and alkaline-treated ITQ-4 zeolites.

Sample	Si/Al_{total} [a]	Si/Al_B [b]	Si/Al_L [b]	$Si_{filtrate}$ [a] (ppm)	$Al_{filtrate}$ [a] (ppm)	V_{total} ($cm^3\ g^{-1}$)	V_{micro} [c] ($cm^3\ g^{-1}$)	S_{meso} [c] ($m^2\ g^{-1}$)	S_{BET} [d] ($m^2\ g^{-1}$)	B_{py}/L_{py} [e]
P	32	42	133	–	–	0.25	0.20	29	529	3.2
AT-2	20	43	38	4240	9	0.41	0.06	206	359	0.9

[a] ICP-OES analysis.
[b] Derived from the Si/Al_{total} and the Brønsted-to-Lewis acid site ratio.
[c] *t*-plot method.
[d] BET method.
[e] Ratio of Brønsted acid sites and Lewis acid sites from infrared of adsorbed pyridine.

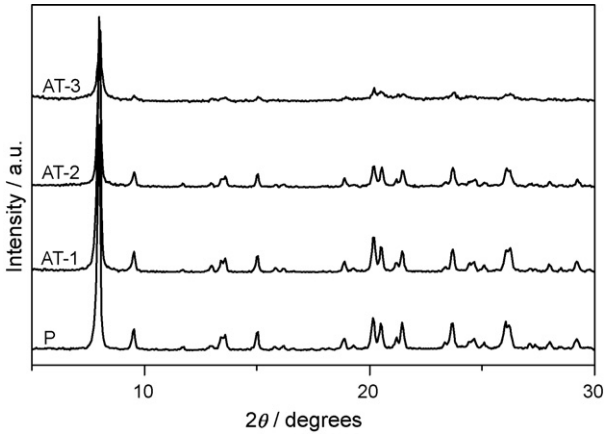

Fig. 2. X-ray diffraction patterns of parent and alkaline-treated ITQ-4 zeolites.

ratio (32) of the calcined zeolite is very close to the ratio in the starting gel (30). The parent zeolite (P) shows the typical diffraction pattern of ITQ-4 as the only crystalline phase (Fig. 2). TEM microscopy shows that the ITQ-4 crystals have beamlike dimensions of 0.2 μm × 0.2 μm × 1.5 μm (Fig. 3a). The N_2 isotherm of P presented a high uptake at low relative pressures, confirming its microporous character (Fig. 4). The textural parameters derived from nitrogen adsorption are collected in Table 1. The micropore volume of ITQ-4 ($V_{micro} = 0.20\ cm^3\ g^{-1}$) is characteristic of the IFR structure [14,19] and accounts for the 80% of the total pore volume. The limited mesoporosity of the parent zeolite ($S_{meso} = 29\ m^2\ g^{-1}$) arises from the crystal's external surface and the surface roughness. The BJH pore size distribution confirmed the absence of any significant mesoporosity (inset of Fig. 4).

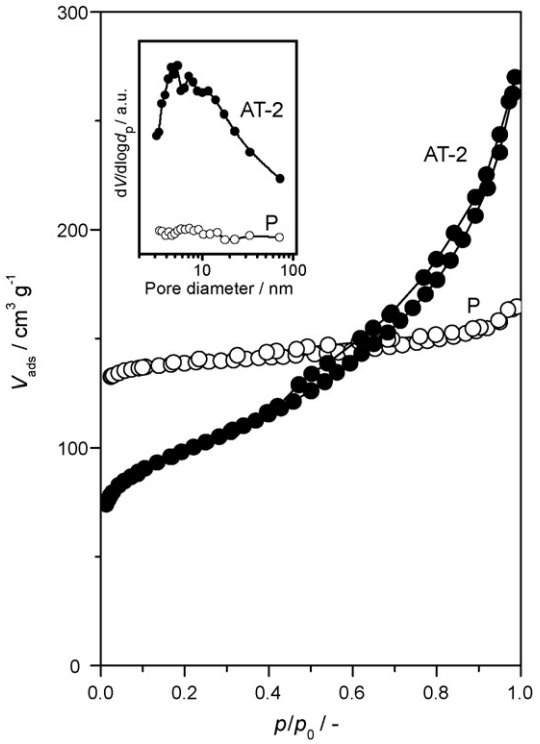

Fig. 4. N_2 isotherms of the parent and alkaline-treated ITQ-4 zeolites. The inset shows the adsorption BJH pore size distributions.

3.2. Mesoporosity development

Upon NaOH treatment the positions of the XRD reflections did not change, indicating the long-range order is generally preserved (Fig. 2). The decrease in intensity of the reflections can be attributed to certain amorphization of the ITQ-4 crystals due to the generation of intracrystalline mesoporosity. The sample treated under severe conditions (AT-3) displays the largest decrease in intensity, which points towards a significant deterioration of the crystal structure. The crystallinity is better preserved in the ITQ-4 samples

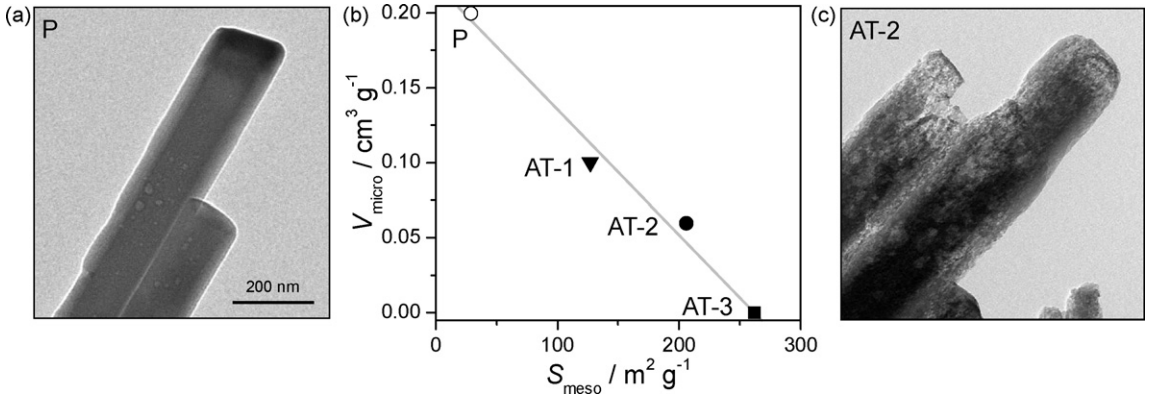

Fig. 3. Influence of the alkaline treatments on the porosity and crystal morphology of ITQ-4. (a) Transmission electron micrograph of the parent sample. (b) Relation of mesoporosity (S_{meso}) and microporosity (V_{micro}) of the parent and alkaline-treated samples. (c) Transmission electron micrograph of alkaline-treated sample.

exposed to mild (AT-1) and standard treatment conditions (AT-2). The gain in mesoporosity is tightly related to the loss in microporosity. Fig. 3b shows that with increasing severity of the treatment the microporous volume decreases linearly with the introduced mesoporosity. Mild treatment (AT-1) resulted in a fourfold increase of the mesoporosity and the loss of 50% of the microporosity. Severe treatment yielded a ninefold increase of the mesoporosity, without any measurable microporosity. We regarded sample AT-2 as the optimal hierarchical lay out for a more detailed study as it combines a sevenfold increase in mesoporosity ($206\,m^2\,g^{-1}$) and a 30% preserved microporosity ($0.06\,cm^3\,g^{-1}$). The TEM image in Fig. 3c clearly visualizes the formation of intracrystalline mesoporosity in AT-2. Mesoporosity is well distributed over the crystals rendering them more transparent and giving the crystals a more brittle appearance. The NaOH treatment on AT-2 resulted in a *ca.* 40% weight loss of the sample and a lower Si/Al ratio (20, Table 1) compared to the parent zeolite. The high Si/Al ratio (*ca.* 500) in the filtrate from the alkaline treatment (Table 1) confirmed that silicon is selectively removed during the alkaline treatment. Nitrogen adsorption demonstrated that the alkaline-treated ITQ-4 samples exhibit uptake at low relative pressures as well as an increased uptake at intermediate pressure (Fig. 4). Sample AT-2 shows a combined type I and type IV isotherm with H3 hysteresis, which is characteristic of a hierarchical porous system combining micro- and mesoporosity [1]. The BJH pore size distribution of AT-2 (inset of Fig. 4) shows a broad distribution mesopores centered around 6 nm.

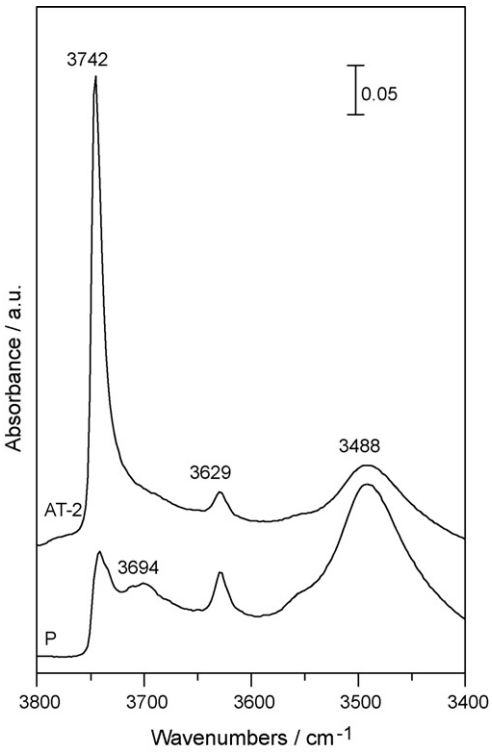

Fig. 5. FTIR spectra in the OH stretching region of the parent and alkaline-treated ITQ-4 zeolites.

3.3. Acidity and accessibility

3.3.1. OH stretching

The infrared spectra in the OH stretching region revealed four absorption bands at 3742, 3700, 3629, and 3488 cm^{-1} (Fig. 5). These bands correspond well with the bands shown for similar IFR-type zeolites reported in [14,20]. The band at 3742 cm^{-1} is typical for the OH stretching vibration of terminal silanols not involved in hydrogen bonding. The band at 3629 cm^{-1} is related to the OH vibration associated with the Brønsted acidity, evidencing the incorporation of Al in the zeolite framework. The assignment of the other two bands is more delicate. These bands were assigned according to previous work [14] and confirmed by the results obtained with the alkaline-treated zeolite (*vide infra*). The low unresolved absorption at 3700 cm^{-1} could be related to extra-framework aluminum hydroxyl groups [20,21]. However, since no relation to the aluminum content was found, we have related this band to hydrogen-bridged silanols which represent framework imperfections [10,14,22]. The band at 3488 cm^{-1} is assigned to hydrogen-bridged forms of the Brønsted-related OH vibrations, which likely result from Brønsted acidic groups in close vicinity of

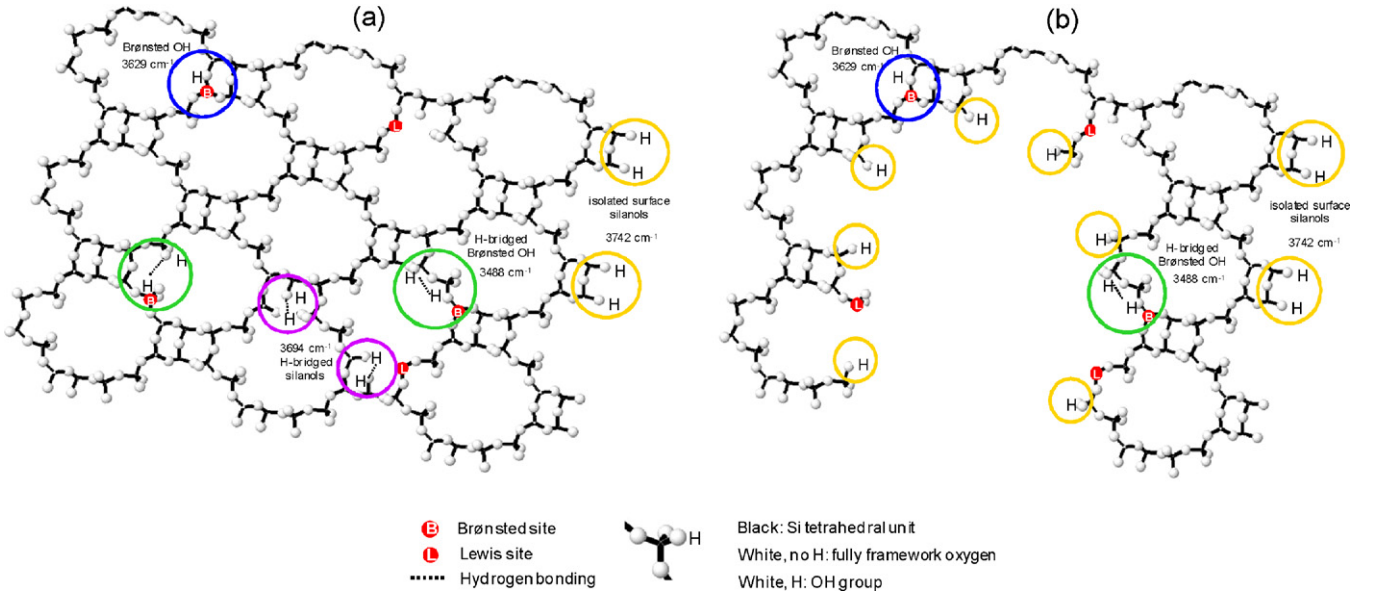

Fig. 6. Schematic representation of the ITQ-4 zeolite's characteristics before and after desilication. (a) 4.5 unit cells of IFR framework with a representative amount of Si and Al. The vibrations observed by infrared spectroscopy in the OH stretching are indicated. (b) The same unit cells after alkaline treatment forming a mesopore. The influence on the Si/Al ratio, Brønsted *versus* Lewis acidity, and the ν_{OH} vibrations can be observed.

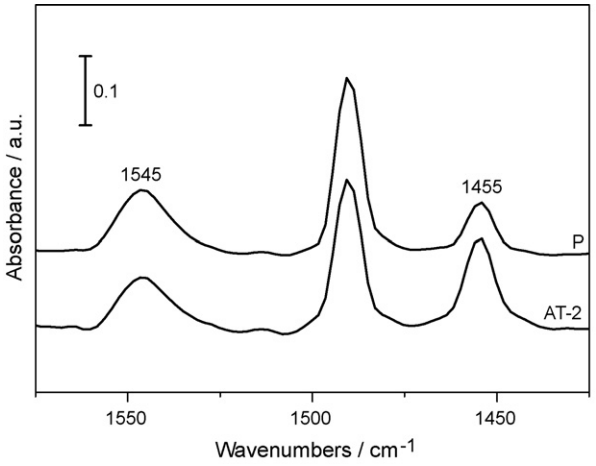

Fig. 7. FTIR spectra of the parent and alkaline-treated ITQ-4 zeolites after adsorption of pyridine.

defective sites [23]. We note that this band has previously been described to a variety of interacting silanol groups or nests [10,24]. Nevertheless, these types of vibrations do not account for the strong correspondence of this band to Brønsted acidic aluminum [14] and were therefore discarded.

The OH stretching region of the alkaline-treated zeolite exemplifies the significant effect of the desilication treatment on ITQ-4. The band at 3742 cm^{-1} assigned to terminal silanols increases dramatically. This is due to partial dissolution of the zeolite framework, hence the formation mesopores, increasing the external surface in the crystals. This agrees well with the increased intracrystalline mesoporosity evidenced by TEM and N_2 adsorption. The small unresolved band at 3700 cm^{-1} turned visibly undistinguishable. As hydroxyl anions preferably attack these framework defects during alkaline treatment [15], it is expected that the intensity of these vibrations reduce strongly upon treatment. The typical Brønsted-related bands at 3629 and 3488 cm^{-1} decreased in intensity, suggesting a change or reduction in Brønsted acidity. This aspect is addressed in the next section. Fig. 6 depicts a visual summary of ITQ-4 zeolite characteristics before (a) and after NaOH treatment (b). The figure illustrates how a possible route to the partial dissolution of the zeolite framework results in a decrease of the Si/Al ratio and the subsequent changes of the OH stretching vibrations of the ITQ-4 zeolite.

3.3.2. Pyridine adsorption

Pyridine adsorption was performed to gain insight into the type and distribution of acid sites in the parent and alkaline-treated ITQ-4 zeolites. The relatively small kinetic diameter (0.57 nm) of pyridine in comparison with the micropore dimensions of ITQ-4 (0.62 nm × 0.72 nm) enables full probing of the intracrystalline acidity. Fig. 7 shows the infrared spectra of pyridine adsorbed on the parent and NaOH-treated samples. The bands at 1545 and 1455 cm^{-1} represent the vibrations associated with pyridine entities adsorbed on Brønsted and Lewis acidic sites, respectively. The integration of these two bands allows to determine their absolute and relative quantities [11,25]. The Brønsted-to-Lewis (B_{py}/L_{py}) ratio (3.2, Table 1) of the parent ITQ-4 indicates that a significant amount of Lewis acidity is present. After NaOH treatment the band at 1455 cm^{-1} increased strongly, whereas the intensity of the band at 1545 cm^{-1} remained constant. Integration of the bands discloses that the B_{py}/L_{py} ratio lowers from 3.2 to 0.9 upon desilication. When combined, the B_{py}/L_{py} ratio and the total amount of aluminum in the zeolites show that the amount of Brønsted sites (Si/Al_B) remains essentially constant whereas the amount of Lewis acidity (Si/Al_L) increases significantly (Table 1). The distribution of acid sites is included in the schematic representation in Fig. 6. The presence of Lewis acidity is of high importance concerning prospective applications in catalysis and adsorption processes. Future work should be directed towards assessing in more depth the nature and role of the created Lewis sites in adsorption and catalysis.

3.3.3. Collidine adsorption

The adsorption of collidine enables to probe the accessibility of the Brønsted acid sites in zeolites as the kinetic diameter of collidine (0.74 nm) exceeds the size of most zeolite micropores [10,11,25]. By monitoring the adsorption of collidine on the ITQ-4 zeolite using infrared spectroscopy, the increased accessibility upon treatment of the parent ITQ-4 zeolite was quantified. The increase in accessibility can be expressed by the amount of adsorbed collidine (A_{coll}) divided by the total amount of acid sites ($B_{py} + L_{py}$), or alternatively, as the amount of adsorbed collidine over the total amount of Brønsted acid sites (B_{py}). In the latter case the assumption is made that collidine does not probe Lewis acid sites. The ($A_{coll}/[B_{py} + L_{py}]$) ratio yields a very small value for the parent zeolite (0.05), which is characteristic to its purely microporous character (inaccessible to collidine). Upon alkaline treatment the ratio increases almost fourfold (to 0.19) for sample AT-2. If we divide the amount of collidine adsorbed on Brønsted sites only, we obtain nearly sixfold increase of the (A_{coll}/B_{py}) ratio, going from sample P (0.07) to sample AT-2 (0.40). Clearly, the use of both approaches proves that the acid site accessibility is remarkably increased in the NaOH-treated sample. The improved accessibility relates to the higher amount of accessible Brønsted sites at the pore mouths of the hierarchical ITQ-4 zeolite due to the newly introduced intracrystalline mesopores.

4. Conclusions

The synthesis of purely microporous and hierarchical ITQ-4 zeolites was successfully carried out. Optimization of the desilication treatment was performed to tune the amount of mesoporosity generated with respect to the loss of micropore volume. The most mesoporous hierarchical zeolite displayed a sevenfold increase in mesoporosity (up to 206 $m^2\,g^{-1}$), combined to a significant loss of crystallinity and a subsequent reduction of *ca.* 70% of microporosity. The Brønsted/Lewis ratio of acidic sites of the parent zeolite equals 3.2. After desilication the Si/Al ratio increased and the Brønsted/Lewis ratio of the hierarchical sample lowered to 0.9. This corresponds to a similar amount of Brønsted acid sites and a higher amount of Lewis acid sites after treatment. Finally, a significant increase in accessibility of the alkaline-treated sample is evidenced. The improved accessibility and altered acidity in the hierarchical ITQ-4 can be anticipated as highly relevance for prospective applications of this zeolite type in catalysis and adsorption processes.

Acknowledgements

This work was funded by the Spanish MICINN (CTQ2009-09824/PPQ, PTQ05-01-00980, Consolider-Ingenio 2010, grant CSD2006-0003) and the ICIQ Foundation. JPR is indebted to the Journal Grants scheme of the Royal Society of Chemistry.

References

[1] J. Pérez-Ramírez, C.H. Christensen, K. Egeblad, C.H. Christensen, J.C. Groen, Chem. Soc. Rev. 37 (2008) 2530.
[2] J.C. Groen, L.A.A. Peffer, J.A. Moulijn, J. Pérez-Ramírez, Colloid Surface A 241 (2004) 53.
[3] X. Wei, P.G. Smirniotis, Micropor. Mesopor. Mater. 97 (2006) 97.
[4] J.C. Groen, T. Sano, J.A. Moulijn, J. Pérez-Ramírez, J. Catal. 251 (2007) 21.
[5] J. Pérez-Ramírez, S. Abelló, L.A. Villaescusa, A. Bonilla, Angew. Chem. Int. Ed. 47 (2008) 7913.

[6] J. Pérez-Ramírez, S. Abelló, A. Bonilla, J.C. Groen, Adv. Funct. Mater. 19 (2009) 164.
[7] A. Bonilla, D. Baudouin, J. Pérez-Ramírez, J. Catal. 265 (2009) 170.
[8] J.C. Groen, J.A. Moulijn, J. Pérez-Ramírez, Micropor. Mesopor. Mater. 87 (2005) 153.
[9] K. Suzuki, Y. Aoyagi, N. Katada, M. Choi, R. Ryoo, M. Niwa, Catal. Today 132 (2008) 38.
[10] M.S. Holm, S. Svelle, F. Joensen, P. Beato, C.H. Christensen, S. Bordiga, M. Bjørgen, Appl. Catal. A 356 (2009) 23.
[11] F. Thibault-Starzyk, I. Stan, S. Abelló, A. Bonilla, K. Thomas, C. Fernandez, J. Gilson, J. Pérez-Ramírez, J. Catal. 264 (2009) 11.
[12] L. Zhao, B. Shen, J. Gao, C. Xu, J. Catal. 258 (2008) 228.
[13] C. Baerlocher, L.B. McCusker, Database of Zeolite Structures, http://www.iza-structure.org/databases.
[14] L.A. Villaescusa, P.A. Barrett, M. Kalwei, H. Koller, M.A. Camblor, Chem. Mater. 13 (2001) 2332.
[15] J.C. Groen, L.A.A. Peffer, J.A. Moulijn, J. Pérez-Ramírez, Chem. Eur. J. 11 (2005) 4983.
[16] S. Brunauer, P.H. Emmett, E. Teller, J. Am. Chem. Soc. 60 (1938) 309.
[17] B.C. Lippens, J.H. de Boer, J. Catal. 4 (1965) 319.
[18] E.P. Barrett, L.G. Joyner, P.P. Halenda, J. Am. Chem. Soc. 73 (1951) 373.
[19] Z. Sarshar, M.H. Zahedi-Niaki, Q. Huang, S. Kaliaguine, Micropor. Mesopor. Mater. 118 (2009) 373.
[20] J. Čejka, A. Krejčí, N. Žilková, J. Kotrla, S. Ernst, A. Weber, Micropor. Mesopor. Mater. 53 (2002) 121.
[21] J.P. Marques, I. Gener, P. Ayrault, J.C. Bordado, J.M. Lopes, F. Ramôa Ribeiro, M. Guisnet, Micropor. Mesopor. Mater. 60 (2003) 251.
[22] T. Blasco, M.A. Camblor, A. Corma, P. Esteve, J.M. Guil, A. Martínez, J.A. Perdigón-Melón, S. Valencia, J. Phys. Chem. B 102 (1998) 75.
[23] C. Pazé, S. Bordiga, C. Lamberti, M. Salvalaggio, A. Zecchina, G. Bellusi, J. Phys. Chem. B 101 (1997) 4740.
[24] F. Pascale, P. Ugliengo, B. Civalleri, R. Orlando, P. D'Arco, R. Dovesi, J. Chem. Phys. 117 (2002) 5337.
[25] N.S. Nesterenko, F. Thibault-Starzyk, V. Montouillout, V.V. Yuschenko, C. Fernandez, J.P. Gilson, F. Fajula, I.I. Ivanova, Micropor. Mesopor. Mater. 71 (2004) 157.